

Comparison of eccentric numerical relativity simulations to small mass-ratio perturbation theory

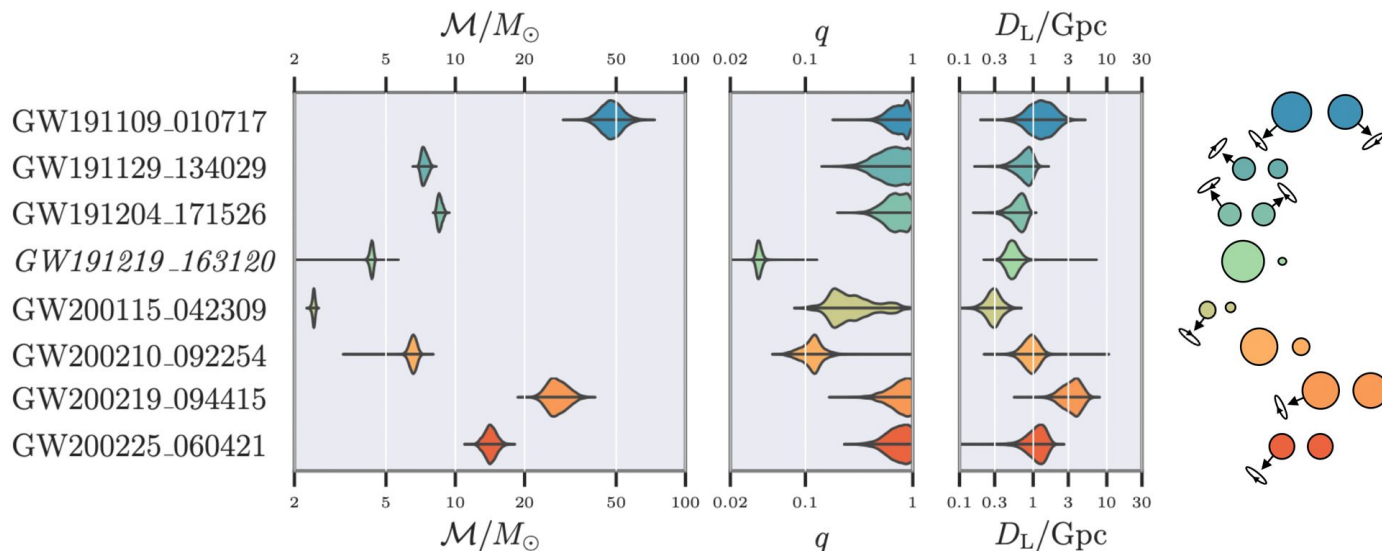
Antoni Ramos-Buades, Harald Pfeiffer and Maarten van de Meent

12th Iberian Gravitational Wave meeting 2022
June 7, 2022



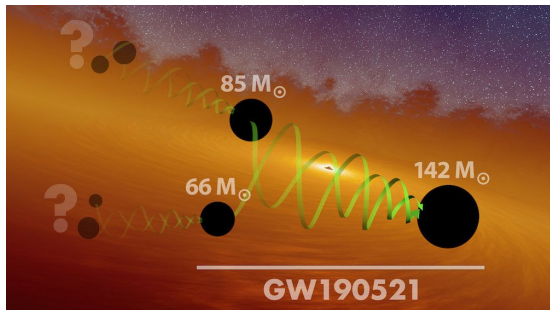
Gravitational-wave detections

- Analysis of the third observing run (O3) recently out (Abbot+2021, Nitz+2021, Olsen+2021).
- Quasi-circular waveform models used in searches and parameter estimation studies.
- Mass-ratio, $Q=m_1/m_2$, for binary black holes (BBHs) mostly consistent with comparable masses.
- In O4 and future detectors, more detections of mass asymmetries as well as eccentric binaries.



Bridging the mass-ratio gap

$q=1$



LVK



Numerical relativity (NR)

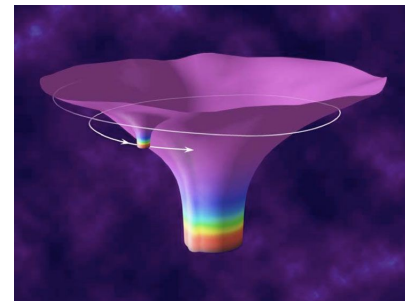
$q \gtrsim 20$



Intermediate mass BH
 $(10 + 1000)M_{\odot}$
 $(10^3 + 10^6)M_{\odot}$

?

$q=0$



EMRI

$(10 + 10^6)M_{\odot}$

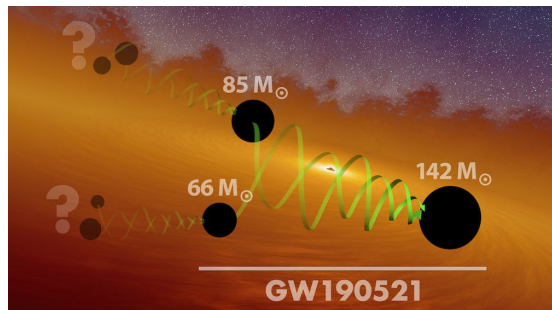


Small-mass-ratio approximation (SMR)

expansion in symmetric mass-ratio $\nu = q / (1+q)^2$

Bridging the mass-ratio gap

$q=1$

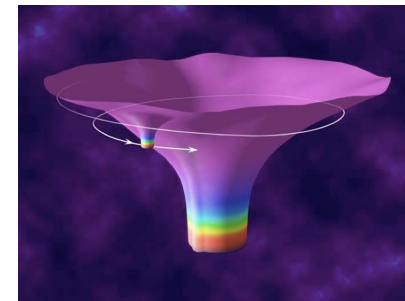


LVK



Intermediate mass BH
 $(10 + 1000)M_{\odot}$
 $(10^3 + 10^6)M_{\odot}$

$q=0$



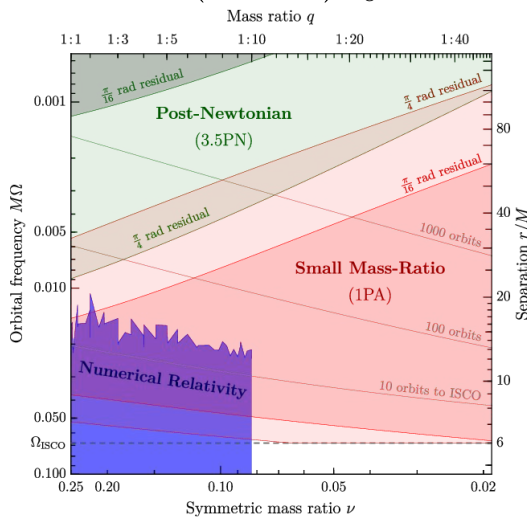
EMRI
 $(10 + 10^6)M_{\odot}$



Numerical relativity (NR)

$q \gtrsim 20$

- Recently [VdMeent&Pfeiffer2020] proposed method to combine information from NR and SMR theory to bridge the gap between both (quasi-circular non-spinning).



Small-mass-ratio approximation (SMR)

expansion in symmetric mass-ratio $\nu = q / (1+q)^2$

- This work extends on eccentric non-spinning BBHs.

Small Mass-Ratio (SMR) evolutions

- Equations of motion as a [perturbative series](#) in [symmetric mass-ratio](#) $\nu = m_1 m_2 / (m_1 + m_2)^2$.
- At [zero-th order](#), just geodesics around Kerr. [Geodesic frequencies](#) are known [analytically](#).

$$\frac{dq_r}{dt} = \Omega_r, \quad \frac{d\phi}{dt} = \Omega_\phi.$$

- At [next order](#) energy [dissipation](#) drives inspiral. [Orbit-averaged fluxes](#) on the right-hand-side are functions of [eccentricity](#), e , and [semi-latus rectum](#), p ,

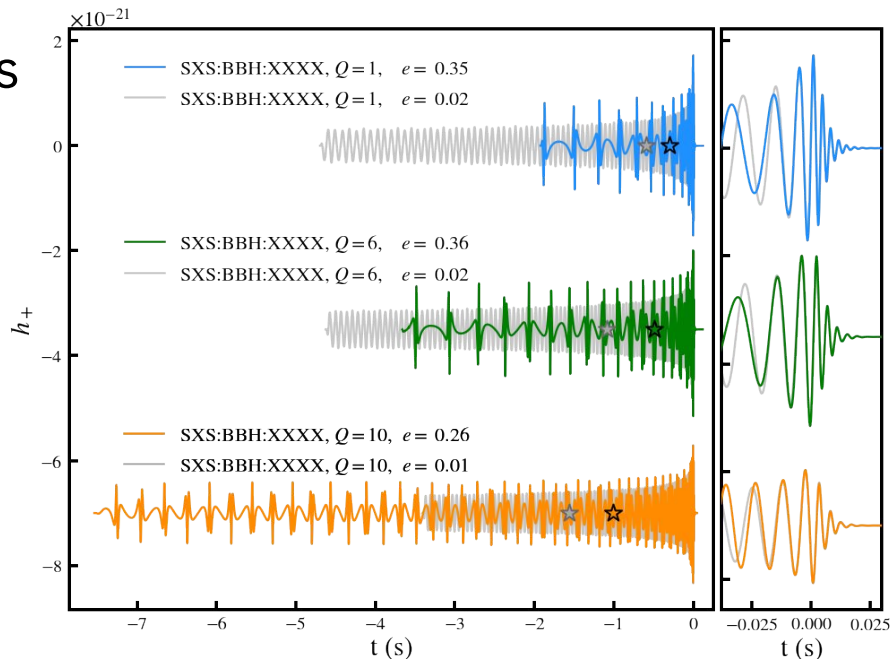
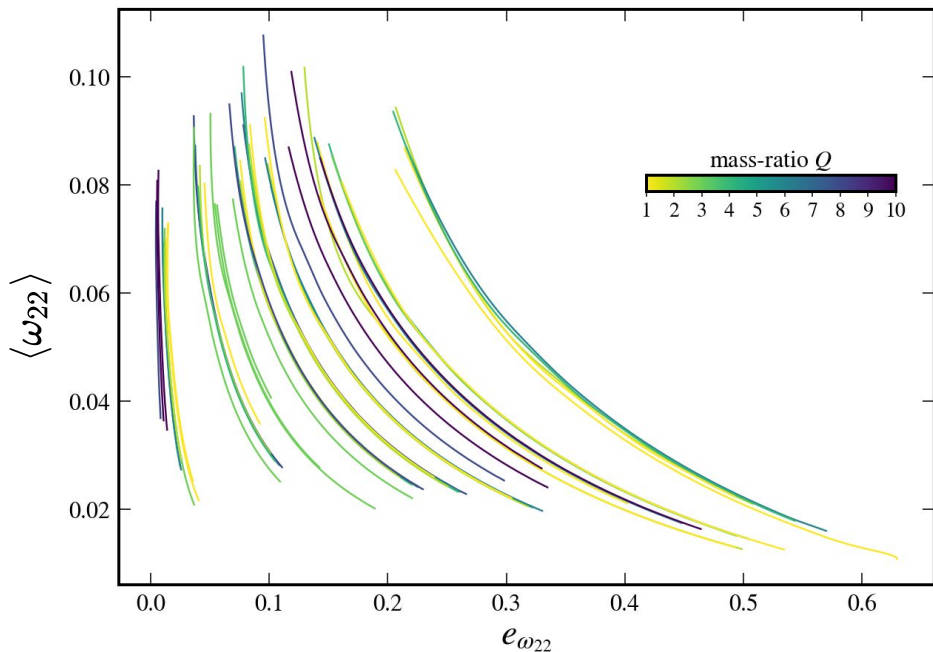
$$\frac{dp}{dt} = \nu \langle F_p \rangle, \quad \frac{de}{dt} = \nu \langle F_e \rangle.$$

- The [fluxes](#) are determined [numerically](#) at any (p, e) value using a [frequency domain Teukolsky code](#).

Numerical Relativity (NR) simulations

- We produced **52 new eccentric non-spinning** simulations with the Spectral Einstein Code (**SpEC**), numerical relativity (NR) code :

$$Q = 1/q = m_1/m_2 = [1 - 10], \quad e_{\omega_{22}} = [0.01 - 0.7]$$



- Long simulations, [20-50] GW cycles.
- 3 different resolutions for each simulation.
- Typical wall clock times:
 - $q=1$: ~ 5-10 days
 - $q=10$: ~ 2-3 months.

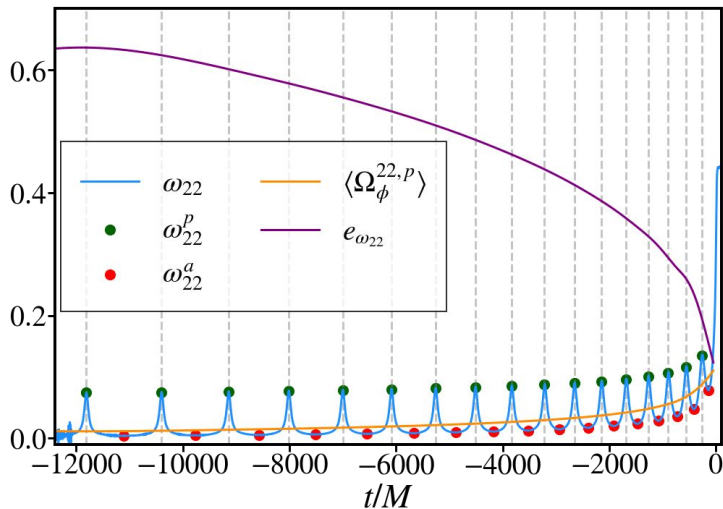
Calculation of frequencies, eccentricity, and fluxes

- Need [coordinate-invariant](#) definition of [eccentricity](#) which is applicable to both NR and SMR.

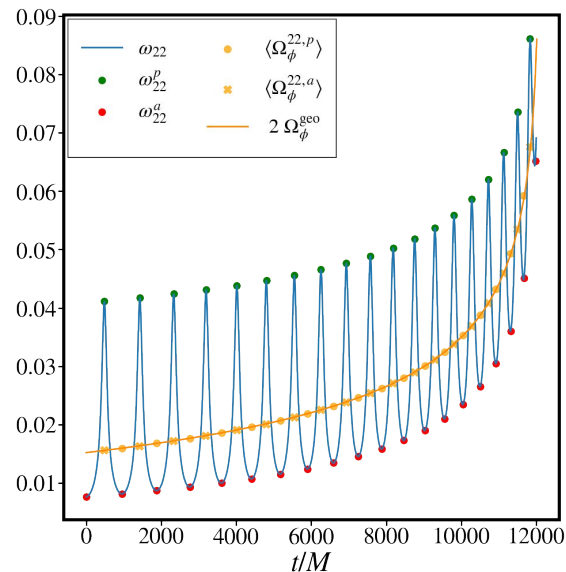
- Define [eccentricity](#) from the [frequency](#) of the quadrupole GW (2,2)-mode. $\omega_{22} = \frac{d}{dt} \text{Arg}[h_{22}(t)]$, $e_{\omega_{22}} = \frac{\omega_{22,p}^{1/2} - \omega_{22,a}^{1/2}}{\omega_{22,p}^{1/2} + \omega_{22,a}^{1/2}}$, $\omega_{22,p}$: ω_{22} at periastron. $\omega_{22,a}$: ω_{22} at apastron.

$$\langle \omega_{22} \rangle \equiv \langle \Omega_{\phi}^{22} \rangle_i = \frac{1}{t_{max}^{i+1} - t_{max}^i} \int_{t_{max}^i}^{t_{max}^{i+1}} \omega_{22}(t) dt, \quad \langle \dot{E}_{GW} \rangle_i = \frac{1}{t_{max}^{i+1} - t_{max}^i} \int_{t_{max}^i}^{t_{max}^{i+1}} \dot{E}_{GW}(t) dt.$$

NR : $m_1/m_2 = 6$



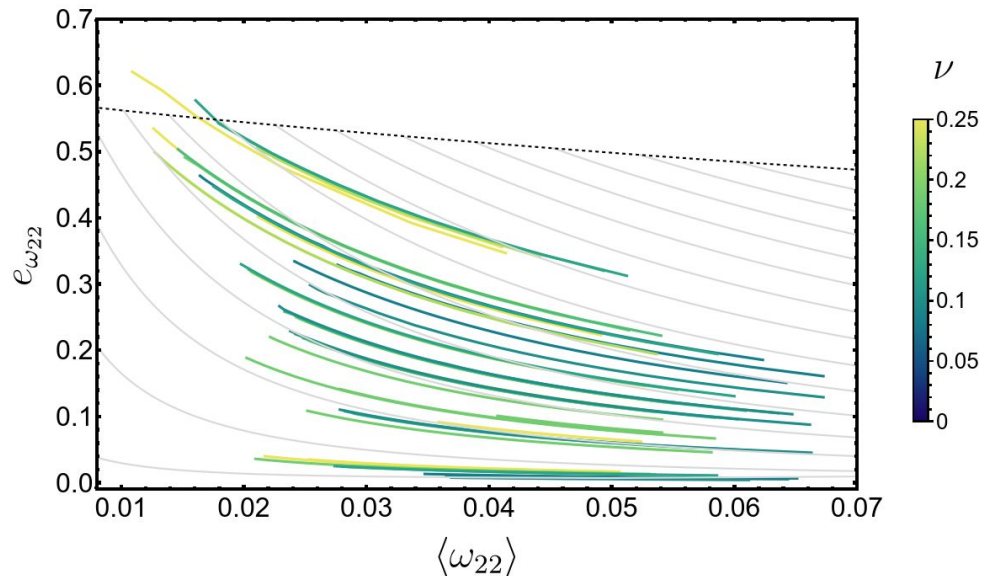
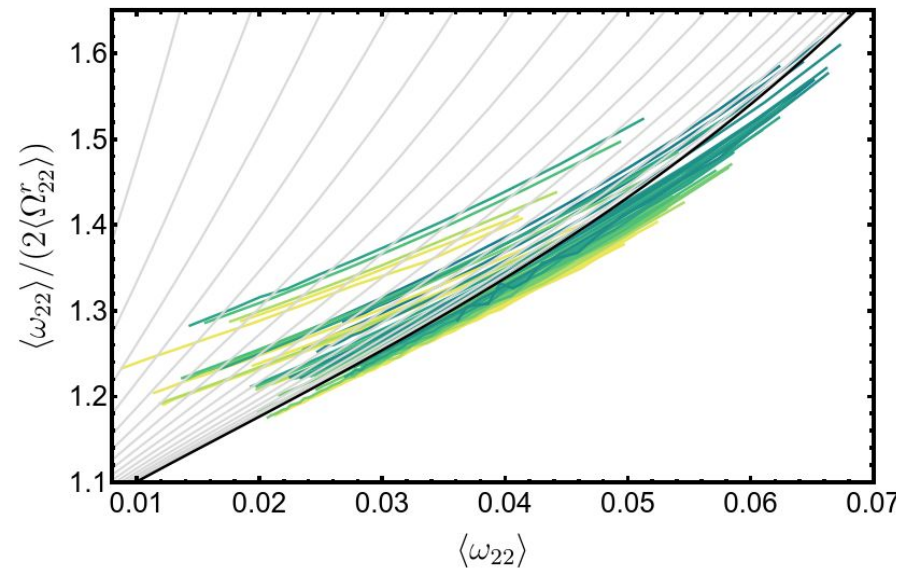
SMR : $m_1/m_2 = 1$



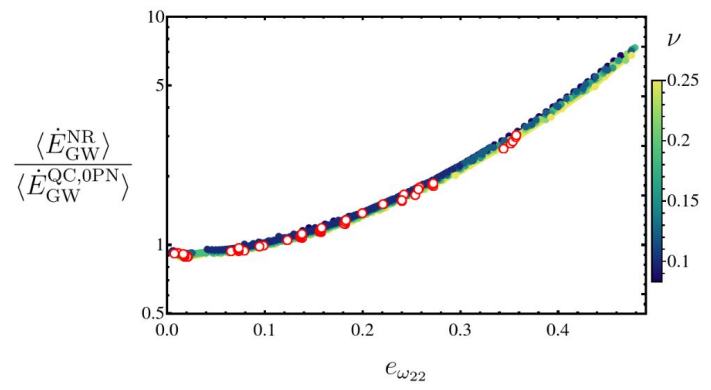
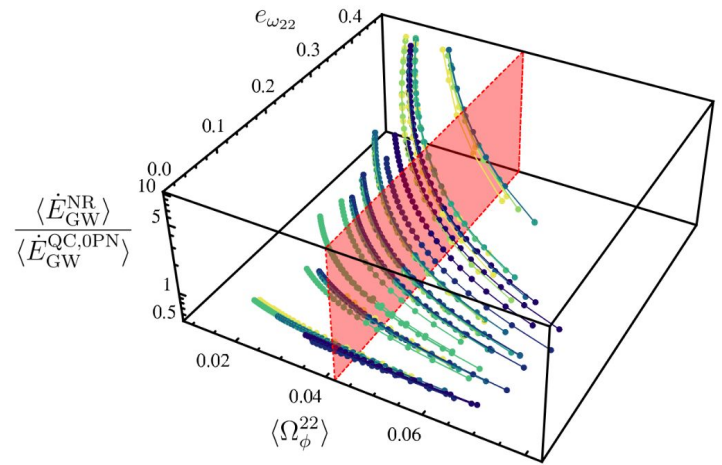
- Use [orbit-average procedure](#) to extract [frequencies](#) and [fluxes](#) from NR simulations [Lewis+2017].
- Also use [periastron-passages](#) to compute additional [orbit-averaged quantities](#).

Comparing NR with SMR

- To compare NR with SMR, one **must map between “NR configuration” and “SMR geodesic”** in a gauge invariant manner.
- The **two characteristic frequencies** (orbital & radial motion) **are not suitable**, because the frequencies of NR often **fall outside the range** spanned by geodesic results.
- We identify NR with SMR by (a) same **orbit-averaged orbital frequency**, $\langle \Omega_\phi^{22} \rangle$, and (b) same **eccentricity** $e_{\omega_{22}}$.



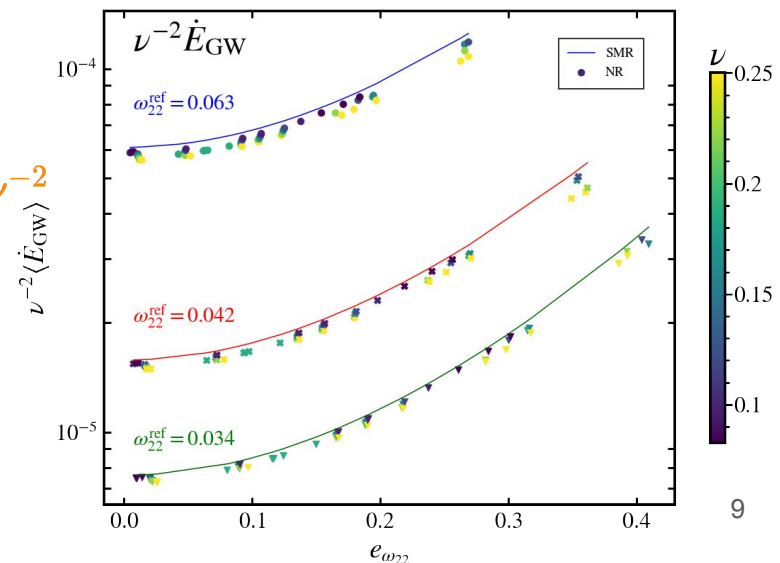
Comparison between SMR and NR results. Energy flux



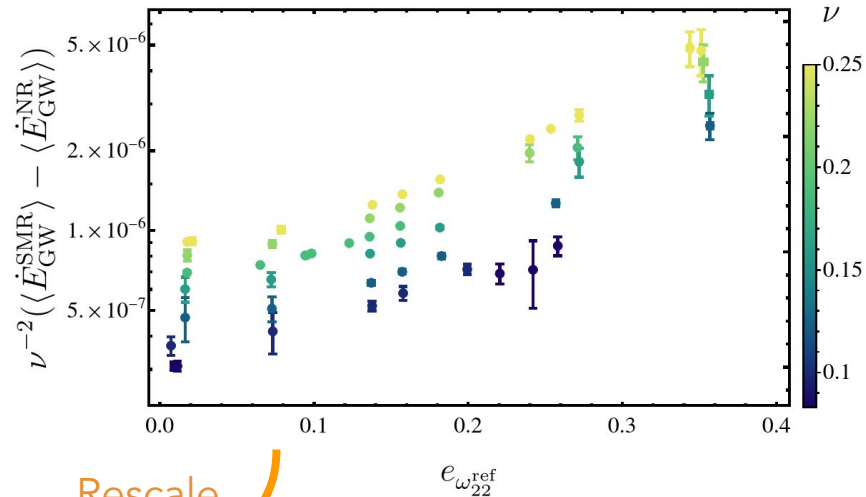
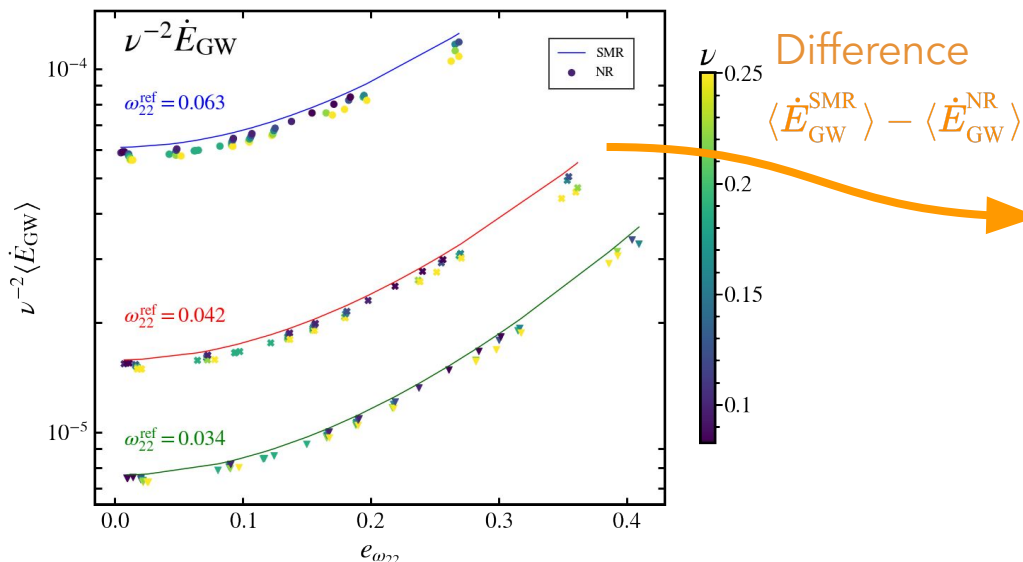
$$\langle \dot{E}_{GW}^{QC,0PN} \rangle = \frac{32}{5} \nu^2 x^5$$

At fixed $\langle \Omega_{22}^{\phi} \rangle_{ref}$,
accounting for $\dot{E} \propto \nu^{-2}$

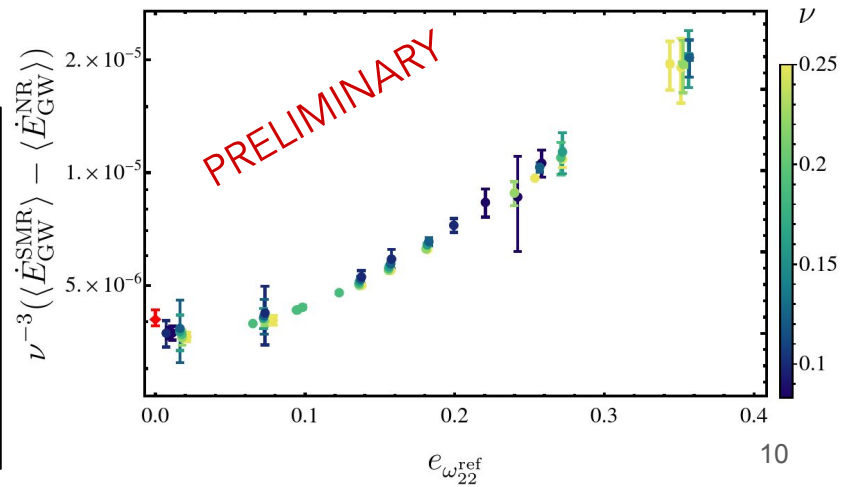
Interpretation:
→ NR and leading-order SMR agree ($\leq 10\%$)
 ν^2 also known as 0-PA



Data at fixed $\langle \Omega_{22}^\phi \rangle_{\text{ref}}$



Rescale
by ν



Interpretation:

→ Collapsed curve gives next-to-leading order contribution

ν^3 also known as 1-PA → *unknown before*

→ Nearly vanishing spread: next-to-next-to-leading-order contribution is small

ν^4 also known as 2-PA → *insignificant*

Conclusions and future work

- Presented new 52 eccentric (≥ 20 orbits) non-spinning simulations with $e_{022} \leq 0.7$ and $Q=[1-10]$.
- Developed tools to map eccentric SMR configurations and NR simulations.
- Analyze energy and angular momentum fluxes, and periastron advance.
- Our NR-SMR comparisons indicate that:
 - At LO 0-PA (v^2) good agreement.
 - At NLO 1-PA (v^3) collapsed curve indicates contribution small (unknown before) \rightarrow NNLO 2-PA (v^4) probably small.